Heterobimetallic Metallaborane Chemistry: Synthesis and Characterization of a "Lightly Stabilized" Molybdairidahexaborane, [{Cp*Ir}{$(CO)_3$(THF)Mo}B_4H_8], and Its Direct Conversion to [{Cp*Ir}{$(CO)_3$(L)Mo}B_4H_8] (L = CO, PPh_3, NCPh, CNBu, NH_3, PPh_3=CHC(O)OMe)

Ramón Macías, Thomas P. Fehlner,* Alicia M. Beatty, and Bruce Noll

Department of Chemistry and Biochemistry, University of Notre Dame, Notre Dame, Indiana 46556-5670

Received September 6, 2004

The reaction of [Cp*IrB_4H_{10}] (**1**) with [{η^6-$(C_6H_4)(CH_3)_2$}Mo$(CO)_3$] in tetrahydrofuran (THF) leads to [Cp*Ir$(CO)_3$(THF)MoB_4H_8] (**2**), which was characterized by NMR spectroscopy. Intermediate **2** subsequently decomposes to give the tetracarbonyl analogue [Cp*Ir$(CO)_4$MoB_4H_8] (**3**). In the presence of free CO, the same reaction constitutes a high-yield synthesis of **3**. The treatment of **2** (formed in situ) with different Lewis bases led to the replacement of the THF ligand at the molybdenum center and generation of [Cp*Ir$(CO)_3$(L)MoB_4H_8] (L = PPh_3 (**4**), NCPh (**5**), CNBu (**6**), NH_3 (**7**)). Reaction of the benzonitrile derivative **5** with PPh_3=$CHCO_2$Me afforded the ylide compound [Cp*Ir$(CO)_3$(PPh_3=$CHCO_2$Me)MoB_4H_8] (**8**). All compounds have been spectroscopically characterized, and **3** and **5**−**7** have been structurally characterized in the solid state. This work demonstrates that, similarly to metal clusters, metallaboranes with labile metal ligands can serve as versatile synthons.

Introduction

Polyhedral boron-containing compounds are uniquely suited for the construction of polymetallic clusters. The frame of a borane or heteroborane provides a matrix on which to bind potentially reactive metal centers. Indeed, stepwise metal attachment to borane frameworks has been used successfully as a synthetic route to polymetallic cluster systems (Chart 1, **I**−**III**).[1−3] Alternatively, polyhedral borane clusters can be used as molecular scaffolds on which to construct polymetallic assemblies. This can be clearly recognized, for example, in the macropolyhedral species [$(PPh_3)_3(PPh_2)_2Pd_4B_{20}H_{16}$],[4] which supports a trimetallic string, or in the recent construction of a {$ReIrAu_2$} butterfly on a rhenacarborane (Chart 1, **IV** and **V**).[5]

In polyhedral boron chemistry, the buildup of polymetallic clusters has relied mainly on the stepwise addition of metal centers to a "preassembled" borane fragment. In the case of carboranes, this has led to the synthesis of many bimetallic and trimetallic compounds.[6−12] In comparison, the parallel development of polymetallic metallaboranes has been much slower.[13−19] This can be attributed in part to the lack of convenient high-yield synthetic methods to metallaboranes. How-

Chart 1. "B-Frames" as Molecular Matrices and Scaffolds: [(Cp*Ir)Co$(CO)_3B_4H_7$] (I),[1] [$(Cp^*Co)_3B_4H_4$] (II),[2] [$(\eta^5$-$C_5H_5)_4Ni_4B_4H_4$] (III),[3] [$(PPh_3)_3(PPh_2)_2Pd_4B_{20}H_{16}$] (IV),[4] and [$(AuPPh_3)_2${Ir$(CO)_3$}{Re$(CO)_2$}(PhC)$B_9H_8$] (V)[5]

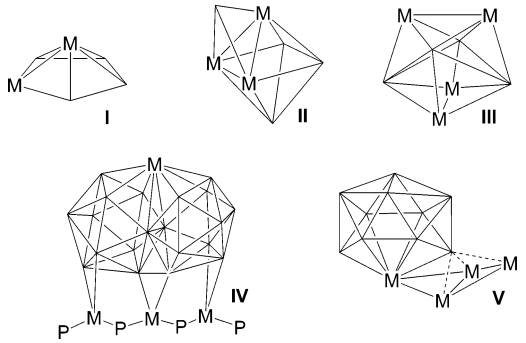

* To whom correspondence should be addressed. E-mail: fehlner.1@nd.edu.

(1) Lei, X.; Shang, M.; Fehlner, T. P. *Chem. Eur. J.* **2000**, *6*, 2653.
(2) Venable, T. L.; Sinn, E.; Grimes, R. N. *Inorg. Chem.* **1982**, *21*, 904.
(3) Bowser, J. R.; Bonny, A.; Pipal, J. R.; Grimes, R. N. *J. Am. Chem. Soc.* **1979**, *101*, 6229.
(4) Yao, H.-J.; Hu, C.-H.; Sun, J.; Jin, R.-S.; Zheng, P.-J.; Bould, J.; Greatrex, R.; Kennedy, J. D.; Ormsby, D. L.; Thornton-Pett, M. *Collect. Czech. Chem. Commun.* **1999**, *64*, 927.
(5) Du, S.; Kautz, J. A.; McGrath, T. D.; Stone, F. G. A. *Angew. Chem., Int. Ed.* **2003**, *42*, 5728.
(6) Mullica, D. F.; Sappenfield, E. L.; Stone, F. G. A.; Woollam, S. F. *J. Chem. Soc., Dalton Trans.* **1993**, 3559.
(7) Grimes, R. N. In *Comprehensive Organometallic Chemistry*; Abel, E. W., Stone, F. G. A., Wilkinson, G., Eds.; Pergamon Press: Oxford, U.K., 1982; Vol. 1.
(8) Grimes, R. N. In *Comprehensive Organometallic Chemistry II*; Abel, E. W., Stone, F. G. A., Wilkinson, G., Eds.; Pergamon: Oxford, U.K., 1995; Vol. 1.
(9) Dossett, S. J.; Hart, I. J.; Stone, F. G. A. *J. Chem. Soc., Dalton Trans.* **1990**, 3481.
(10) Ellis, D. D.; Jelliss, P. A.; Stone, F. G. A. *Dalton* **2000**, 2113.
(11) Ellis, D. D.; Jeffery, J. C.; Jelliss, P. A.; Kautz, J. A.; Stone, F. G. A. *Inorg. Chem.* **2001**, 2041.
(12) Carr, N.; Mullica, D. F.; Sappenfield, E. L.; Stone, F. G. A.; Went, M. J. *Organometallics* **1993**, *12*, 4350.
(13) Kennedy, J. D. *Prog. Inorg. Chem.* **1984**, *32*, 519.
(14) Kennedy, J. D. *Prog. Inorg. Chem.* **1986**, *34*, 211.

10.1021/om049308f CCC: $27.50
Publication on Web 11/03/2004

ever, this situation changed with the development of a general route to a class of metallaboranes derived from mono(cyclopentadienyl)metal chlorides.[20] The majority of compounds prepared from this route contain two metal centers ranging from groups 5 to 9. Thus, the availability of (homo)bimetallic metallaboranes opens an attractive alternative to earlier methods for the construction of polymetallic clusters.

In this regard, mixed-metal clusters of the group 6 metallaboranes have been prepared in high yield by controlled cluster expansion reactions with metal carbonyls $M_2(CO)_8$ (M = Fe, Co).[1,21] However, reports of clusters containing early−late metals that differ by three d-block groups are scarce and little is known of their reactivity.[22] These mixed-metal clusters are of interest because the presence of a polar metal−metal bond could lead to interesting chemistry via cooperative M−M' interactions. It has been already demonstrated that the hybrid character of a metallaborane creates reaction possibilities not seen for transition-metal complexes or boranes individually.[23,24] For example, it has been suggested that heterobimetallic metal hydrides possessing both hydridic M−H bonds and acidic M−H bonds are potentially excellent reducing agents.[25,26] Thus, metallaboranes in which an early transition metal is bound to a late transition metal are good candidates for hydrogenation catalysts. Here we describe the reaction of [Cp*IrB_4H_9] (**1**) with the molybdenum complex [η^6-(xylene)$Mo(CO)_3$]. Subsequent substitution reactions at the molybdenum center of the labile initial product afford a significant series of molybdairidaborane derivatives. These mixed-metal clusters represent the first examples of Mo−Ir heterobimetallic metallaboranes.

Results and Discussion

Reaction of [Cp*IrB_4H_{10}] (1) with [{η^6-$C_6H_4(CH_3)_2$}$Mo(CO)_3$]. We discovered that in the early stages of the reaction of the iridapentaborane **1** with stoichiometric amounts of (η^6-xylene)tricarbonylmolybdenum the molybdairidahexaborane [1-Cp*-2,2,2-$(CO)_3$-2-(THF)-*nido*-1,2-$IrMoB_4H_8$] (**2**) (Scheme 1) is formed. In solution, this bimetallic metallaborane decomposes, giving the tetracarbonyl analogue [1-Cp*-2,2,2,2-$(CO)_4$-*nido*-1,2-$IrMoB_4H_8$] (**3**) in modest yields.

Scheme 1

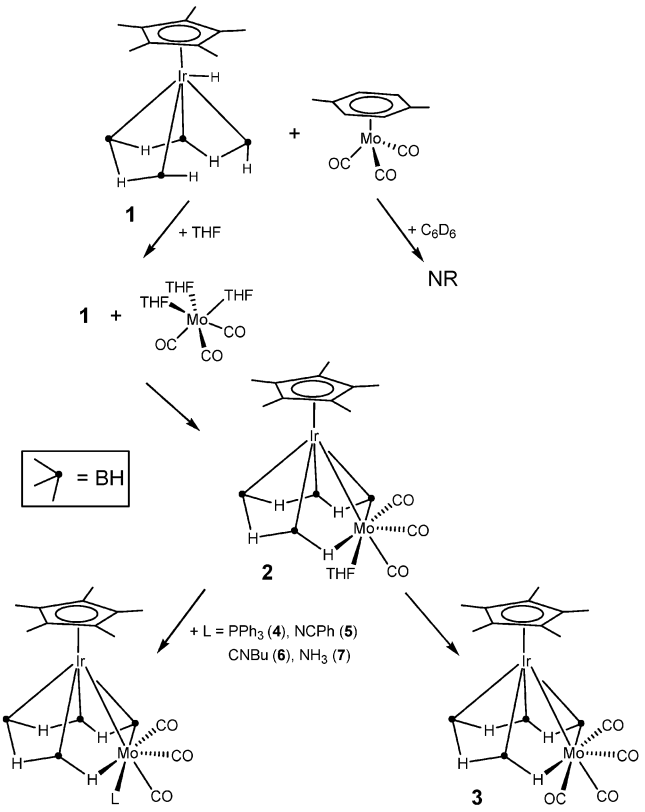

Compound **3** was sufficiently stable to allow its purification by column chromatography on silica gel. The orange product was characterized by ^1H and ^{11}B NMR spectroscopy, X-ray diffraction analysis, and additional standard techniques. In contrast, the unstable tetrahydrofuran derivative **2** could be characterized only by NMR spectroscopy in solution.

Metal fragment addition to a metallaborane is a common approach to the buildup of clusters. Similarly, the formation of compound **2** involves the addition of a {$Mo(CO)_3$(THF)} group to the five-vertex *arachno*-iridapentaborane **1** and elimination of H_2. The reaction can be viewed as a formal substitution of the apical Ir−H hydride and one BH hydrogen atom of the {B_4H_9} fragment by the molybdenum center.

In tetrahydrofuran, the reaction between **1** and the (arene)tricarbonylmolybdenum complex to give **2** was completed in about 30 min, depending on the concentration of the reactants, and was accompanied by the generation of gas presumed to be H_2. In contrast, in benzene the iridapentaborane did not react with the molybdenum complex and both reactants were recovered unchanged. This suggests that arene displacement by THF is necessary for the reaction to proceed. In fact, dissolution of (η^6-arene)$Mo(CO)_3$ in THF or acetone leads to rapid loss of the arene (minutes or less) and solvent addition to generate $(L)_3Mo(CO)_3$ (L = acetone, THF).[27]

It is probable that $(THF)_3Mo(CO)_3$ is the species that reacts with **1** (Scheme 1). The complete mechanism is unclear, but displacement of THF by a hydride of **1** from $(THF)_3Mo(CO)_3$ that generates a metallaborane inter-

(15) Barton, L., Strivastava, D. K. In *Comprehensive Organometallic Chemistry II*; Abel, E. W., Stone, F. G. A., Wilkinson, G., Eds.; Pergamon: New York, 1995; Vol. 1.
(16) Bould, J.; Crook, J. E.; Greenwood, N. N.; Kennedy, J. D.; McDonald, W. S. *J. Chem. Soc., Chem. Commun.* **1983**, 949.
(17) Bould, J.; Crook, J. E.; Kennedy, J. D. *Inorg. Chim. Acta* **1993**, *203*, 193.
(18) Kim, Y.-H.; Cooke., P. A.; Greatrex, R.; Kennedy, J. D.; Thornton-Pett, M. *J. Organomet. Chem.* **1998**, *550*, 341.
(19) Kim, Y.-H.; McKinnes, Y. M.; Cooke, P. A.; Greatrex, R.; Kennedy, J. D.; Thornton-Pett, M. *Collect. Czech. Chem. Commun.* **1999**, *64*, 938.
(20) Fehlner, T. P. *Organometallics* **2000**, *19*, 2643.
(21) Aldridge, S.; Shang, M.; Fehlner, T. P. *Inorg. Chem.* **1998**, *37*, 928.
(22) Lucas, N. T.; Blitz, J. P.; Petrie, S.; Stranger, R.; Humphrey, M. G.; Heath, G. A.; Otieno-Alego, V. *J. Am. Chem. Soc.* **2002**, *124*, 5139.
(23) Hong, Y.; Beatty, A. M.; Fehlner, T. P. *J. Am. Chem. Soc.* **2002**, *124*, 10280.
(24) Hong, Y.; Beatty, A. M.; Fehlner, T. P. *J. Am. Chem. Soc.* **2003**, *125*, 16367.
(25) Casey, C. P.; Wang, Y.; Tanke, R. S.; Hazin, P. N.; Rutter, E. W., Jr. *New J. Chem.* **1994**, *18*, 43.
(26) Bullock, R. M.; Casey, C. P. *Acc. Chem. Res.* **1987**, *20*, 167.
(27) Muetterties, E. L.; Bleeke, J. R.; Sievert, A. C. *J. Organomet. Chem.* **1979**, *178*, 197.

Scheme 2

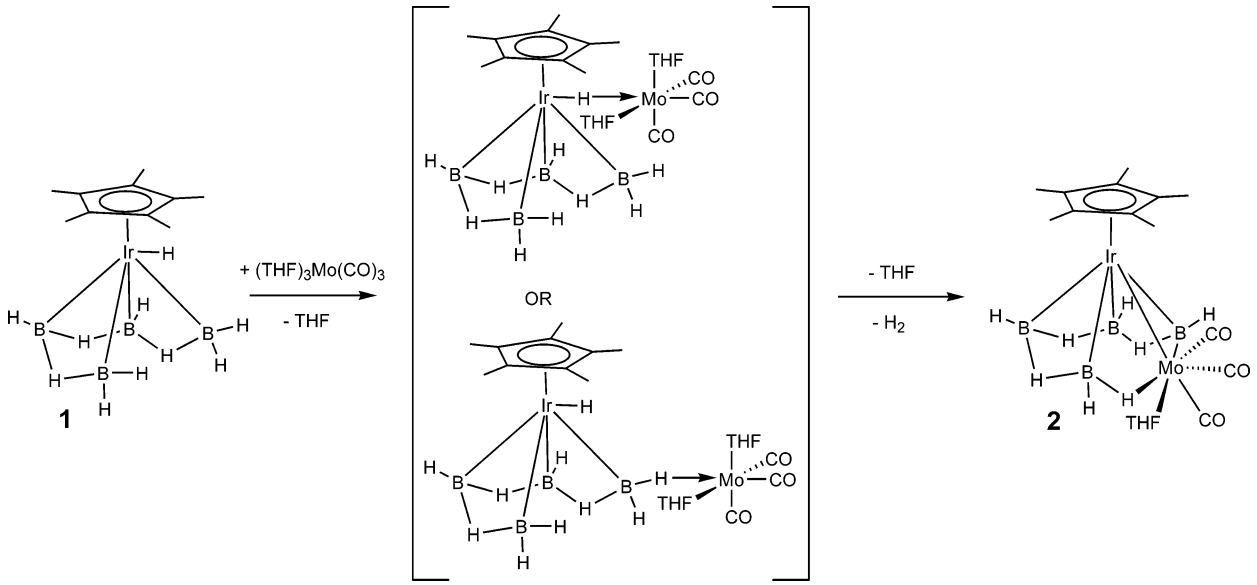

mediate that can undergo cluster insertion and unimolecular elimination of H_2 (Scheme 2) is an attractive pathway.

Since the isolated yield of **3** is less than 50%, it is likely that the formation of this metallaborane involves the addition of a CO molecule generated from decomposition of the THF derivative (eq 1). Consistent with

$$2[\mathrm{Cp^*Ir(CO)_3(THF)MoB_4H_8}] \rightarrow \underset{\mathbf{2}}{} \underset{\mathbf{3}}{[\mathrm{Cp^*Ir(CO)_4MoB_4H_8}]} + \ldots \quad (1)$$

this hypothesis, the addition of CO gas to the reaction system leads to higher (67%) yields of **3**. Hence, **2** can be viewed as a "lightly stabilized" metallaborane and suggests that other Lewis bases should efficiently generate a series of related mixed metal derivatives.

Substitution Reactions at the Molybdenum Center. A variety of Lewis bases were found capable of replacing the THF ligand in compound **2** (Scheme 1). In a typical reaction, the iridapentaborane **1** was treated with stoichiometric amounts of $[\{\eta^6\text{-}C_6H_4(Me)_2\}Mo(CO)_3]$ to give $[\{Cp^*Ir\}\{(CO)_3(THF)Mo\}B_4H_8]$ (**2**). When the formation of **2** was complete, as judged by NMR, the appropriate Lewis base was added. This synthetic procedure led to series of molybdairidahexaboranes of the general formula $[\{Cp^*Ir\}\{(CO)_3(L)Mo\}B_4H_8]$ (L = PPh_3 (**4**), NCPh (**5**), CNBu (**6**), NH_3 (**7**)).

Substitution of the THF ligand took place at room temperature in a few minutes. The benzonitrile and butyl isocyanide derivatives **5** and **6** were purified by column chromatography on silica gel, whereas the ammonia counterpart was isolated by crystalization in CH_2Cl_2/hexane at −40 °C. The products were characterized by NMR spectroscopy, mass spectrometry, and elemental analysis. We also determined the crystal structures of compounds **3** and **5**−**7** (Tables 1 and 2).

Compounds **5** and **7** decomposed in solution under argon at +4 °C overnight, giving a brown precipitate and the tetracarbonyl derivative **3**. However, both species were crystallized from CH_2Cl_2/hexane at −40 °C, affording products that were stable for long periods of time as solids. Furthermore, these crystalline compounds can be handled in air. The PPh_3 analogue also decomposed in solution, but at slower rates. In contrast, the CNBu derivative is stable in solution and in the solid state and its stability resembles that of the tetracarbonyl compound **3**.

Like compound **2**, the benzonitrile analogue **5** undergoes substitution at the molybdenum center. In contrast to the THF derivative, which can only be generated in situ, **5** can be isolated in crystalline stable form. Therefore, **5** gives better control of stoichiometry in reactivity studies. In addition, **5** is less reactive than **2** in an overall sense and more selective, thereby allowing the synthesis of species that otherwise would not be accessible from compound **2**.

For example, the reaction between **2** and the carbonyl-stabilized phosphorus ylide $Ph_3P{=}CHCO_2Me$ resulted in a complex mixture from which we could not identify or isolate any new compounds. In contrast, the treatment of **5** with the same reagent afforded a new metallaborane that we identified as [1-Cp*Ir-2,2,2-$(CO)_3$-2-(PPh_3CHCO_2Me)-*nido*-1,2-$IrMoB_4H_8$] (**8**) but were unable to completely separate from **3**. $Ph_3P{=}CHCO_2Me$ behaves as a weak nucleophile capable of replacing the benzonitrile ligand. Similar reactivity was previously observed for $[PdCl_2(NCPh)_2]$ in the formation of the substitution product $[PdCl_2(PPh_3CHCO_2Me)_2]$.[28,29]

Structures of 5−7. The structures of **3** and **5**−**7** were established by X-ray crystallography, and a summary of the crystallographic data and selected bond distances and angles for **5**−**7** are given in Tables 1 and 2, respectively. The structure solution of compound **3** gave a residual peak of 21 e $Å^{-3}$ near Ir that could not be modeled satisfactorily; therefore, the molecular metrics are uncertain. However, the X-ray diffraction data are sufficient to confirm the molecular connectivity of **3** and show it to be a member of the series.

A typical structure of the series can be seen in Figure 1, which shows the molecular structure of **7**. These

(28) Vicente, J.; Chicote, M. T.; Fernandez-Baeza, J. *J. Organomet. Chem.* **1989**, *364*, 407.
(29) Weleski, E. T., Jr.; Silver, J. L.; Jansson, M. D.; Burmeister, J. L. *J. Organomet. Chem.* **1975**, *102*, 365.

Table 1. Experimental X-ray Diffraction Parameters and Crystal Data for [{Cp*Ir}{(CO)$_4$Mo}B$_4$H$_8$] (3), [{Cp*Ir}{(CO)$_3$(NCC$_6$H$_5$)Mo}B$_4$H$_8$] (5), [{Cp*Ir}{(CO)$_3$(CNBu)Mo}B$_4$H$_8$] (6), and [{Cp*Ir}{(CO)$_3$(NH$_3$)Mo}B$_4$H$_8$] (7)

	3	5	6	7
empirical formula	$C_{14}H_{23}B_4IrMoO_4$	$C_{20}H_{28}B_4IrMoNO_3$	$C_{18}H_{32}B_4IrMoNO_3$	$C_{13}H_{26}B_4IrMoNO_3$
fw	586.70	661.81	641.83	575.73
cryst dimens (mm)	0.50 × 0.32 × 0.04	0.69 × 0.43 × 0.03	0.30 × 0.16 × 0.06	0.28 × 0.10 × 0.07
space group	$P2_1/c$	$C2/c$	$Pbca$	$P2_1/c$
a, Å	16.8242(8)	29.2740(6)	13.7651(3)	8.7480(3)
b, Å	11.9429(5)	10.5875(2)	13.8575(3)	26.1356(11)
c, Å	19.9351(9)	17.3862(4)	24.5446(5)	8.6082(3)
α, deg	90	90	90	90
β, deg	103.9170(10)	119.8180(10)	90	108.253(2)
γ, deg	90	90	90	90
V, Å^3	3888.0(3)	4675.24(17)	4681.88(17)	1869.10(12)
Z	8	8	8	4
D(calcd), g cm^{-3}	2.005	1.880	1.821	2.046
μ(Mo Kα), mm^{-1}	7.496	6.244	6.232	7.792
temp, K	100(2)	100(2)	100(2)	100(2)
$2\theta_{max}$, deg	56	66	63	66
transmissn factors	1.0000−0.6000	0.8495−0.0997	0.6986−0.2590	0.653−0.468
no. of rflns collected	41 601	60 441	35 279	28 786
no. of obsd rflns ($I > 2\theta(I)$)	9670	8813	6231	6302
no. of params refined	433	308	347	246
R	0.0612	0.0328	0.0227	0.0272
R_w	0.1498	0.0854	0.0493	0.0598
goodness of fit	1.052	1.024	1.033	1.082
largest peak in final diff map, e/Å^3	20.787	3.160	1.233	3.797

Table 2. Selected Interatomic Lengths (Å) and Angles (deg) for [{Cp*Ir}{(CO)$_3$(NCC$_6$H$_5$)Mo}B$_4$H$_8$] (5), [{Cp*Ir}{(CO)$_3$(CNBu)Mo}B$_4$H$_8$] (6), and [{Cp*Ir}{(CO)$_3$(NH$_3$)Mo}B$_4$H$_8$] (7)

	5	6	7
	Lengths		
Ir(1)−Mo(2)	2.8521(2)	2.8566(2)	2.8534(3)
Ir(1)−B(3)	2.146(3)	2.140(3)	2.146(4)
Ir(1)−B(6)	2.096(3)	2.095(3)	2.099(3)
Mo(2)−B(3)	2.476(3)	2.460(4)	2.470(4)
Mo(2)−B(6)	2.287(3)	2.293(3)	2.270(3)
Mo(2)−C(1)	1.926(3)	1.954(3)	1.927(3)
Mo(2)−C(2)	1.980(3)	1.955(4)	1.960(3)
Mo(2)−C(3)	2.007(3)	2.001(3)	2.013(3)
Mo(2)−E[a]	2.210(2)	2.177(3)	2.297(3)
C(1)−O(1)	1.180(3)	1.164(3)	1.177(4)
C(2)−O(2)	1.146(3)	1.159(4)	1.151(4)
C(3)−O(3)	1.146(3)	1.144(4)	1.140(4)
N−C	1.145(3)	1.192(7)	
B(3)−B(4)	1.831(5)	1.836(5)	1.825(5)
B(4)−B(5)	1.824(5)	1.815(5)	1.825(5)
B(5)−B(6)	1.847(4)	1.846(5)	1.855(5)
	Angles		
B(3)−Mo(2)−B(6)	81.19(10)	81.09(12)	92.88(14)
B(4)−B(3)−Mo(2)	115.23(17)	115.5(2)	116.6(2)
C(1)−Mo(2)−E[a]	163.31(10)	159.12(12)	161.58(14)
B(3)−Mo(2)−C(2)	146.67(10)	145.03(12)	145.87(14)
Ir(1)−Mo(2)−C(3)	169.96(8)	172.34(14)	173.60(10)
Mo(2)−N−C	174.3(2)		
Mo(2)−C−N		160.0(5)	
C(1)−Mo(2)−C(2)	90.44(11)	90.93(13)	90.71(15)
C(1)−Mo(2)−C(3)	76.05(11)	78.17(13)	78.83(14)
C(2)−Mo(2)−E	93.65(10)	94.93(14)	96.97(13)
C(3)−Mo(2)−E	87.88(11)	82.06(12)	85.06(13)
B(3)−Mo(2)−E	79.87(9)	81.06(13)(	77.81(12)
B(6)−Mo(2)−C(3)	135.79(11)	137.50(13)	136.87(14)
Mo(2)−C(1)−O(1)	172.5(2)	171.1(2)	172.3(3)
Mo(2)−C(2)−O(2)	177.4(3)	177.0(3)	177.6(3)
Mo(2)−C(3)−O(3)	173.3(3)	175.3(3)	174.5(3)
B(6)−Mo(2)−E	135.26(9)	138.93(11)	136.98(12)

[a] E = N for **5** and **7**, and E = C for **6**.

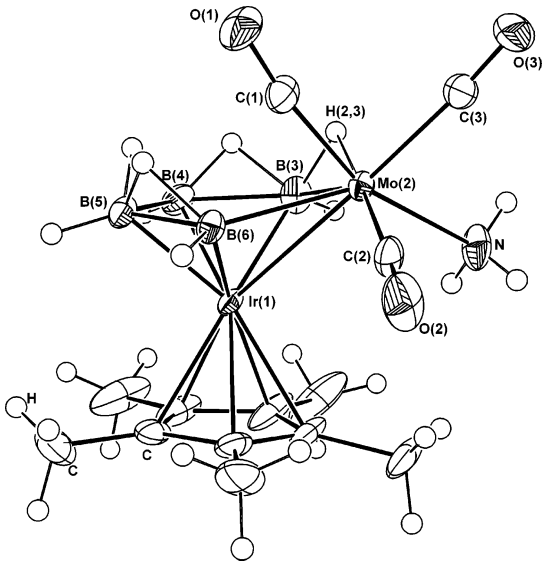

Figure 1. Molecular structure of **7**, the NH_3 derivative.

molydairidaboranes have a {1-Ir-2-Mo-B$_4$} pentagonal-pyramidal core geometry (Chart 1, **I**). The framework structures correspond exactly to what one expects for an eight-SEP, six-vertex nido cluster.[30] The Ir−Mo bond distances are very similar within the series, being slightly longer for compound **6**. The {Mo(CO)$_3$L} fragment (L = NCPh (**5**), CNBu (**6**), NH_3 (**7**)) binds in an asymmetric fashion within the cluster. Thus, the Mo(2)−B(3) length is significantly longer than the Mo(2)−B(6) distance (0.152(4) Å average difference). This difference is consistent with the presence of a bridging hydrogen atom at the Mo(2)−B(3) edge, resulting in a longer Mo−B interaction. In contrast, the Ir(1)−B(3) edge is only slightly longer than the Ir(1)−B(6) edge with an average difference within the series of 0.047(4) Å.

The Mo(2)−C(1) bond corresponds to the carbonyl that is trans to the L ligand. In the benzonitrile and ammonia (**5** and **7**) derivatives the length of this bond is slightly shorter (0.027(3) Å) than in the isocyanide analogue **6**; conversely, the C(1)−O(1) distances are

(30) Wade, K. *Adv. Inorg. Chem. Radiochem.* **1976**, *18*, 1.

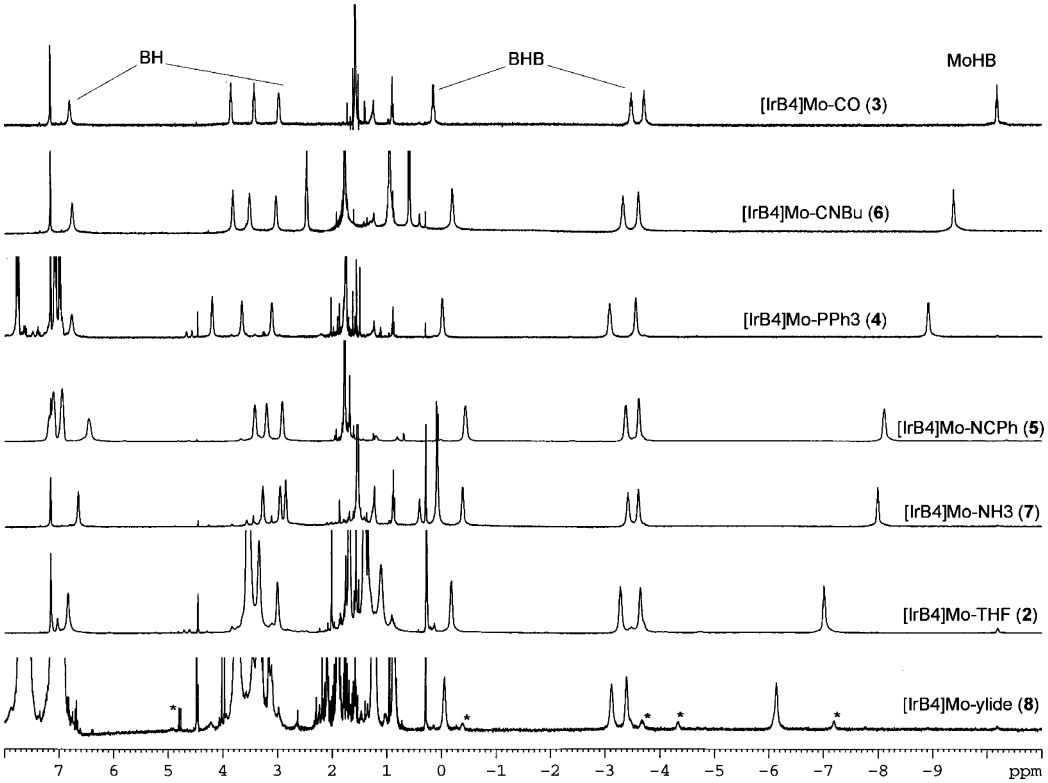

Figure 2. $^{1}H\{^{11}B\}$ NMR spectra.

slightly longer for the former pair of compounds. In addition, in comparison with NCPh, the CNBu ligand exhibits a longer C−N distance (0.047(7) Å), which suggests that the latter displays stronger π-acceptor character.

The angle between the L group and the *trans*-carbonyl ligand C(1)O(1) is close to 160° throughout the series; the carbonyl faces the pentagonal face of the cluster, and the L ligand is cis to the bridging hydrogen bond, H(2,3). In all the species, the carbonyl, C(2)O(2), is almost trans to this bridging hydrogen atom, and the third carbonyl, C(3)O(3), forms an angle close to 170° with the iridium center. This stereochemistry can be rationalized on the basis of 6-coordinate octahedral molybdenum, in which the metal is a formally saturated 18-electron center. This implies bonding vectors toward the B(3)H(2,3) bond and the Ir(1)B(6) edge of the iridapentaborane fragment in addition to the four terminal ligands.

When they are viewed as metal complexes, these bimetallic metallahexaboranes can be regarded as featuring either a Mo(0) center bound to a four-electron neutral η^3-Cp*IrB_4H_8 ligand or a Mo(II) center linked to an anionic six-electron η^3-Cp*$IrB_4H_8^{2-}$ fragment (i.e. isolectronic with *arachno*-$B_5H_9^{2-}$). Since the iridapentaborane fragment formally replaces two THF molecules of the starting $(THF)_3Mo(CO)_3$ to give compound **2**, and the $(CO)_3LMo$ group formally substitutes two hydrogen atoms from [Cp*IrB_4H_{10}] (**1**), both descriptions are notionally valid. The description of the Cp*IrB_4H_8 fragment as a 4-electron bidentate ligand is consistent with a 6-coordinate octahedral center, whereas a 6-electron tridentate Cp*IrB_4H_8 fragment implies a 7-coordinate Mo center.

NMR Characterization. The NMR data of the molybdairidaboranes in solution are fully in accord with the solid-state structures of compounds **3** and **5**−**7**. The $^{11}B\{^{1}H\}$ NMR spectra consist of four signals of relative intensity 1, indicating that the C_s symmetry is maintained. Of the four boron resonances, one appears at around 45 ppm for all compounds and is at significantly lower field than the other three signals lying between 10 and −5 ppm. The ^{1}H NMR spectra also reflect the asymmetry of the compounds (Figure 2)

Scheme 3. Proposed Fluxional Process in [2,2,2-$(CO)_3$-*nido*-2-FeB_5H_9]

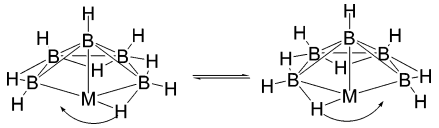

The molybdairidaboranes have the same bridging hydrogen configuration as the ferrahexaborane [2,2,2-$(CO)_3$-*nido*-2- FeB_5H_9];[31] however, the latter exhibits a dynamic behavior at ambient temperature, in which the Fe−H−B bridging hydrogen atom moves between the B(3)−Fe(2) and B(6)−Fe(2) edges of the pentagonal face (Scheme 3). In contrast, variable-temperature NMR experiments demonstrated that compound **3** is not fluxional, even at 100 °C in toluene-d_8. Even the $Mo(CO)_4$ group is static, as the ^{13}C NMR shows four distinct carbonyl resonances at room temperature.

In the series, eight different proton resonances associated with boron atoms are observed. One of the BH terminal ^{1}H resonances appears near the aromatic region. The other three terminal BH resonances occur between 4 and 3 ppm. Four signals around 0 ppm and in the negative region of the ^{1}H spectra correspond to the bridging hydrogen atoms. The resonance at highest

(31) Shore, S. G.; Ragaini, J. D.; Smith, R. L.; Cottrell, C. E.; Fehlner, T. P. *Inorg. Chem.* **1979**, *18*, 670.

field is reasonably assigned to the MoHB hydrogen atom. $^1H\{^{11}B\}$ selective experiments permit correlation of the lowest field BH_t proton resonance with the lowest field ^{11}B signal and the ^{11}B resonance at around 9 ppm with the MoHB hydrogen atom. Hence, these two boron resonances are assigned to cluster positions B(6) and B(3), respectively (Figure 1).

A comparison of the proton cluster resonances (Figure 2) reveals that the MoHB signal shifts significantly through the series from the highest field resonance of the tetracarbonyl derivative to the lowest field signal of the ylide and THF species. Interestingly, the compounds that are more stable in solution (i.e. **3** and **6**) exhibit the MoHB resonance at the highest field, whereas for the least stable species (i.e. **2** and **8**) the resonance shifts to low fields. The MoHB resonance correlates with the stability of the corresponding metallahexaborane relative to ligand displacement or loss.

In compound **2**, the THF resonances were assigned to the broad signals at 3.68 and 1.52 ppm. The NH_3 ligand of **7** led to a broad peak at 0.09 ppm assigned to NH protons, which in toluene-d_8 shifted from 0.20 ppm at 29 °C to −0.15 ppm at −60 °C. In the ^1H and ^{31}P NMR spectra of the Mo−ylide complex **8**, the resonances of the methine proton and the phosphorus atom shift to lower field on coordination. This change is consistent with coordination of the ylide ligand to the molybdenum center. As the NMR data of the coordinated ylide ligand is similar to that found in the palladium complex $\{PdCl_2(PPh_3HCC(O)Me)_2\}$,[28,29] we propose that the ylidic carbon binds the molybdenum atom. However, the ylidic electron pair is delocalized and therefore either the carbon or the oxygen can act as donors. Inspection of the $^1H\{^{11}B\}$ NMR spectrum at the bottom of Figure 2 reveals that there are weak signals (indicated as asterisks) in the negative region of the spectrum that can be assigned to a second $\{Mo(CO)_3L\}$ derivative. Note that the shift of the MoHB resonance in this presumed coordination isomer is close to that of the THF compound **2**. This is consistent with coordination of the ylide via the carbonyl oxygen atom rather than the methine carbon atom. However, without definitive structural data, the bonding mode of the ligand remains uncertain.

Comparison of the IR Spectra. The average CO stretching frequency decreases by 83 cm^{-1} on moving through the series from the tetracarbonyl derivative **3** to the ammonia analogue **7** (Figure 3). The band at the highest frequency shifts by 9 cm^{-1} to lower values, whereas the band with the lowest wavenumber suffers a significant shift of 46 cm^{-1} from **3** to **7**. However, the greatest ν_{CO} shifts toward low frequencies are observed when one carbonyl is substituted by CNBu and then by PPh_3. In particular, either the band at 1976 or 1968 cm^{-1} in **6** shifts a minimum of 84 and 76 cm^{-1}, respectively, to lower values when the isocyanide ligand is substituted by PPh_3.

Significantly, the order of decreasing average frequency for the five compounds is exactly the same as found for the MoHB chemical shift. Decreasing CO frequency is an accepted measure of increasing negative charge buildup on the metal center. Hence, it appears that replacement of the fourth CO of the $Mo(CO)_4$ fragment with increasingly poorer π-acceptor ligands

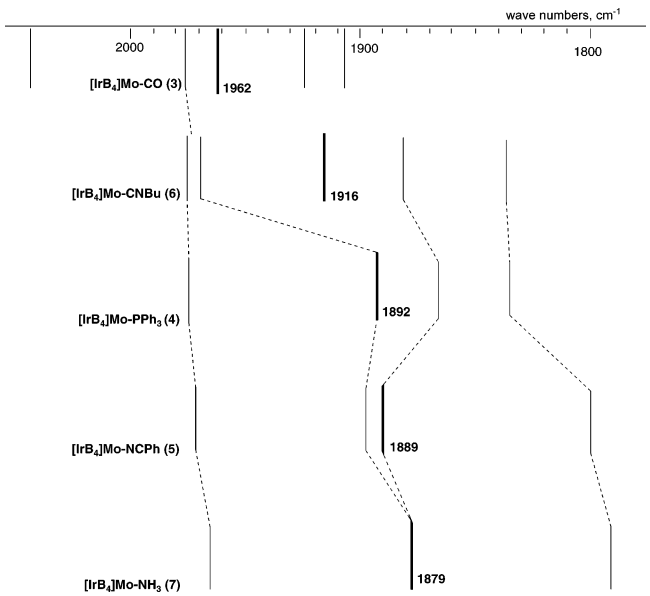

Figure 3. Representation of the IR spectra. The average frequencies are given in boldface type, which for the PPh_3, NCPh, and NH_3 derivatives coincide with one of the spectral bands. The dotted lines do not imply assignments and illustrate only frequency shifts.

leads to charge buildup and correspondingly more facile ligand loss.

This different degree of Mo−CO "back-bonding" conforms with the slight elongation of the C(1)−O(1) bond that is observed when the C≡NBu trans ligand in **6** is replaced by N≡CPh or NH_3 in **5** and **7**, respectively.

Conclusions

The synthesis of "lightly stabilized" metallaboranes **2** and **3** has allowed the systematic study of substitution reactions at a molybdenum center incorporated into an iridaborane framework. The series of derivatives generated provides the first spectroscopic and structural data for mixed-metal Mo−Ir metallaboranes. The substitution chemistry can be extended to other Lewis bases, affording controlled functionalization of the {MoIrB} hybrid core and concomitant change of the electronic contributions of the Mo metal. The molybdenum fragment in **2** and **5** is a reactive center with potential cooperative effects between the adjacent boron and iridium atoms. Reactions with organic substrates may lead to the synthesis of new hybrid clusters and/or to useful transformations of the organic reagents.

Experimental Section

General Considerations. All reactions were carried out under an argon atmosphere using standard Schlenk-line techniques.[32] Solvents were distilled immediately before use under a dinitrogen atmosphere: sodium benzophenone ketyl for hexanes and tetrahydrofuran and calcium hydride for dichloromethane. All commercial reagents were used as received without further purification. The iridapentaborane **1** and the (arene)tricarbonylmolybdenum complex were prepared by following synthetic procedures previously reported.[1,33] NMR

(32) Shriver, D. F., Drezdzon, M. A. *The Manipulation of Air-Sensitive Compounds*; Wiley-Interscience: New York, 1986.
(33) Pidcock, A.; Smith, J. D.; Taylor, B. W. *J. Chem. Soc. A* **1967**, 872.

spectra were recorded on a 400 MHz Bruker instrument. NMR references: internal (C_6D_6, δ_H 7.16 ppm) for ^1H; external ([$(Me_4N)(B_3H_8)$] in acetone-d_6, δ_B −29.7 ppm) for ^{11}B; external (H_3PO_4 in D_2O, δ_P 0.0 ppm) for ^{31}P. IR spectra were recorded on a Nicolet 205 FT-IR spectrometer. Mass spectra were acquired on a Finnigan MAT Model 8400 mass spectrometer. M-H-W Laboratories, Phoenix, AZ, performed elemental analysis.

X-ray Structure Determinations. The crystallographic details of **3** and **5**−**7** are gathered in the Supporting Information. All data were collected on a Bruker Apex CCD diffractometer at 100(2) K with Mo Kα radiation (λ = 0.710 73 Å). Relevant data for the crystallographically studied compounds are summarized in Table 1.

Reaction of [Cp*IrB$_4$H$_{10}$] (1) with [{η^6-(C$_6$H$_4$)(CH$_3$)$_2$}-Mo(CO)$_3$]. Method 1: Without Free CO. A 36 mg portion of the iridapentaborane **1** was treated with 27 mg (0.094 mmol) of the molybdenum complex in 4 mL of tetrahydrofuran. The solution became bright yellow; then, a few minutes later, it turned to orange, and finally it changed to brown and became cloudy with a suspension. The reaction mixture was filtered through silica gel to give a bright brown solution (the silica gel retained a brown residue). The solvent was evaporated and the residue examined by NMR in C_6D_6 and characterized as compound **2**.

[{Cp*Ir}{(THF)(CO)$_3$Mo}B$_4$H$_8$] (**2**): ^{11}B NMR (C_6D_6) δ 44.7 (br. d, ^1J(B,H) = 137 Hz, 1B), 9.5 (br, 1B), −5.0 (br d, 2B); $^1H\{^{11}B\}$ NMR (C_6D_6) δ 6.95 (s, 1H, BH$_t$), 3.68 (br, THF), 3.63 (s, 1H, BH$_t$), 3.45 (s, 1H, BH$_t$), 3.12 (s, 1H, BH$_t$), 1.80 (s, 15H, Cp*), 1.52 (br, THF), 0.28 (s, 1H, BHB), −3.17 (s, 1H, BHB), −3.54 (s, 1H, BHB), −6.90 (s, 1H, MoHB).

After the characterization of **2** by NMR spectroscopy, the solvent was removed under vacuum, the red-brown residue dissolved in hexane, and this solution applied to a chromatography column. Using hexane as eluent, we isolated an orange band that we characterized as [1-Cp*-2,2,2,2-(CO)$_4$-*nido*-1,2-IrMoB$_4$H$_8$] (**3**; 14 mg, 0.027 mmol, 29%). IR (cyclohexane): 2523 (w br, ν_{BH}), 2488 (w br, ν_{BH}), 2465 (w br, ν_{BH}), 2042 (s, ν_{CO}), 1976 (s, ν_{CO}), 1922 (s, ν_{CO}), 1906 (s, ν_{CO}). LR-MS (FAB): *m/z* 587 (M^+), calcd for $C_{14}H_{23}O_4B_4IrMo$; found envelope with cutoff at *m/z* 563 and maximum at 558 {M^+ − (CO + H)}, and the loss of three consecutive CO molecules. Anal. Calcd for $C_{14}H_{23}O_4B_4IrMo$: C, 28.66; H, 3.95. Found: C, 28.86; H, 4.12. ^{11}B NMR (C_6D_6): δ 51.7 (d, ^1J(B,H) = 137 Hz, 1B), 9.7 (t, ^nJ(B,H) = 76 Hz, 1B), −3.2 (d, ^1J(B,H) = 155 Hz, 1B), −5.4 (d, ^1J(B,H) = 151 Hz, 1B). $^1H\{^{11}B\}$ NMR (C_6D_6): δ 6.81 (s, BH$_t$), 3.85 (t, ^nJ(H,H) = 7 Hz, BH$_t$), 3.42 (t, ^nJ(H,H) = 6 Hz, BH$_t$), 2.97 (m, BH$_t$), 1.66 (s, 15H, Cp*), 0.14 (q, ^nJ(H,H) = 6 Hz, 1H, BHB), −3.38 (quit, ^nJ(H,H) = 8 Hz, 1H, BHB), −3.62 (quit, ^nJ(H,H) = 8 Hz, 1H, BHB), −10.08 (t, ^nJ(H,H) = 7 Hz, 1H, MoHB). $^{13}C\{^1H\}$ NMR ($C_6D_5CD_3$): δ 217.6 (CO), 217.3 (CO), 212.3 (CO), 208.1 (CO), 99.4 (C_5Me_5), 8.9 ($C_5(CH_3)_5$).

Method 2: With Free CO. A 48 mg portion (0.17 mmol) of [η^6-(xylene)Mo(CO)$_3$] was added to a solution of 65 mg (0.17 mmol) of **1** in THF under an argon atmosphere. The reaction mixture was stirred at room temperature for 30 min. Following this, CO was bubbled through the solution at room temperature for 1 h. The resulting bright orange solution was evaporated to dryness, affording an orange residue. The latter was dissolved in hexane and transferred to the top of a chromatography column packed with silica gel. Elution with neat hexane gave an orange fraction. Removal of solvent in vacuo yielded **3** as an orange powder (65 mg, 0.11 mmol, 67%).

Synthesis of [{Cp*Ir}{(CO)$_3$(PPh$_3$)Mo}B$_4$H$_8$] (4). To 28 mg (0.07 mmol) of **1** dissolved in 5 mL of THF, we added the molybdenum complex at room temperature under an atmosphere of argon. The initial pale yellow solution of the iridapentaborane turned to bright orange and then to brown-orange. After 5 min of stirring, the THF was evaporated to give a brown residue, which was dissolved in CH_2Cl_2 and filtered through silica gel. The resulting bright orange solution was treated with 19 mg (0.07 mmol) of PPh_3 to give a bright red mixture, which was stirred for 1 h at room temperature. Then, the solvent was evaporated to dryness and the residue extracted with hexane. The hexane solution was refrigerated at 4 °C, and overnight red star-shaped crystals were isolated. The NMR of the remaining residue (after extraction with hexane) showed the peaks of **1**, $BH_3{\cdot}PPh_3$, and the iridatriborane and iridatetraborane adducts [Cp*IrB$_2$H$_6$(PPh$_3$)] and [Cp*IrB$_3$H$_7$(PPh$_3$)].[34] The red crystals were characterized as [1-Cp*-2,2,2-(CO)$_3$-2-PPh$_3$-*nido*-1,2-IrMoB$_4$H$_8$] (**4**, 14 mg, 0.02 mmol, 29%). IR (KBr): 2522 (m, ν_{BH}), 2504 (m, ν_{BH}), 2456 (m, ν_{BH}), 2427 (m, ν_{BH}), 1975 (s, ν_{CO}), 1892 (vs, ν_{CO}), 1865 (vs, ν_{CO}), 1837 (sh, ν_{CO}). HR-MS (FAB): *m/z* 823.1536 (M^+ − H), calcd for $C_{31}H_{38}O_3B_4IrPMo$; measd *m/z* 823.1562. Anal. Calcd for $C_{31}H_{38}O_3B_4IrPMo$: C, 45.35; H, 4.67. Found: C, 45.25; H, 4.71. ^{11}B NMR (C_6D_6): d 51.2 (br, 1B), 11.0 (br, 1B), −4.3 (br, 2B). $^1H\{^{11}B\}$ NMR (C_6D_6): δ 7.78−7.76 (6 H, PPh), 7.16−6.94 (9 H, PPh), 6.77 (s, 1H, BH$_t$), 4.20 (s, 1H, BH$_t$), 3.66 (s, 1H, BH$_t$), 3.11 (s, 1H, BH$_t$), 1.75 (s, 15H, Cp*), −0.01 (s, 1H, BHB), −3.08 (s, 1H, BHB), −3.56 (s, 1H, BHB), −8.92 (s, 1H, MoHB). $^{31}P\{^1H\}$ NMR (C_6D_6): δ 54.7 (s).

Synthesis of [{Cp*Ir}{(CO)$_3$(NCPh)Mo}B$_4$H$_8$] (5). A 38 mg portion (0.1 mmol) of **1** was treated with 29 mg (0.1 mmol) of [{η^6-1,2-(CH$_3$)$_2$-C$_6$H$_4$}Mo(CO)$_3$] in 1.5 mL of THF. A 5-fold excess of benzonitrile was added, and the reaction mixture was stirred for 30 min at room temperature under argon. The solvent was evaporated to dryness, yielding an orange-yellow residue, which was chromatographed on a silica gel column. Elution with hexane/CH_2Cl_2 (1:1) afforded a yellow band that was crystallized from hexane/CH_2Cl_2 to give, after drying under vacuum, 50 mg (0.07 mmol) of [1-Cp*-2,2,2-(CO)$_3$-2-(NCC$_6$H$_5$)-*nido*-1,2-IrMoB$_4$H$_8$] (**5**; 70% yield). IR (KBr): 2958 (w, ν_{CH}). 2915 (w, ν_{CH}), 2516 (m, ν_{BH}), 2464 (m, ν_{BH}), 2250 (w, ν_{NC}), 1971 (s, ν_{CO}), 1897 (s, ν_{CO}), 1889 (s, ν_{CO}), 1798 (s, ν_{CO}), 1589 (w, ν_{CC}), 1442 (w, ν_{CC}), 1377 (w, ν_{CC}). LR-MS (FAB): *m/z* 662 (M^+), calcd for $C_{20}H_{28}O_3B_4NIrMo$; found weak envelope with cutoff at *m/z* 666 and maximum at *m/z* 659 {M^+ − 3(H)}, strong envelope with cutoff at *m/z* 639 and maximum at *m/z* 634 that corresponds to {M^+ − CO}. Anal. Calcd for $C_{20}H_{28}O_3B_4NIrMo$: C, 36.29; H, 4.26. Found: C, 36.37; H, 4.41. $^{11}B\{^1H\}$ NMR (C_6D_6; peaks are too broad to resolve the ^nJ(B,H) coupling): δ 46.3 (s, 1B), 8.9 (s, 1B), −4.8 (s, 1B), −5.2 (s, 1B). $^1H\{^{11}B\}$ NMR (C_6D_6): δ 7.05−6.95 (m, 1H, C_6H_5CN), 6.80−6.75 (m, 2H, C_6H_5CN), 6.65−6.58 (m, 2H, C_6H_5CN), 6.91 (s, 1H, BH$_t$), 3.69 (s, 1H, BH$_t$), 3.45 (s, 1H, BH$_t$), 3.12 (s, 1H, BH$_t$), 1.77 (s, 15H, Cp*), −0.07 (q, ^nJ(H,H) = 7 Hz, 1H, BHB), −3.27 (quit, ^nJ(H,H) = 7 Hz, 1H, BHB), −3.45 (s, 1H, BHB), −8.10 (t, ^nJ(H,H) = 7 Hz, 1H, MoHB).

Synthesis of [{Cp*Ir}{(CO)$_3$(CNBu)Mo}B$_4$H$_8$] (6). We treated 0.1064 g (0.279 mmol) of **1** with 0.08 g (0.279 mmol) of the molybdenum complex in 4 mL of THF at room temperature under argon. After 30 min of stirring, we added 0.14 mL (1.395 mmol) of butyl isocyanide. The brown solution was stirred for another 30 min. The solvent was evaporated to dryness, and the brown residue was dissolved in CH_2Cl_2 to give a bright yellow solution, which was filtered off through silica gel under an argon atmosphere. The silica gel retained a brown residue, and the filtrate gave a yellow solution. Evaporation of the dichloromethane under vacuum afforded a yellow residue that was crystallized in hexane to give 81 mg (45% yield) of the yellow iridamolybdahexaborane [1-Cp*-2,2,2-(CO)$_3$-2-(CNBu)-*nido*-1,2-IrMoB$_4$H$_8$] (**6**). IR (KBr): 2959 (w, ν_{CH}), 2913 (w, ν_{CH}), 2873 (w, ν_{CH}), 2515 (m, ν_{BH}), 2460 (m, ν_{BH}), 2189 (s, ν_{CN}), 1976 (vs, ν_{CO}), 1968 (vs, ν_{CO}), 1882 (vs, ν_{CO}), 1836 (vs, ν_{CO}). HR-MS (FAB): *m/z* 644.1360 (M^+ − H), calcd for $C_{18}H_{31}O_3NB_4IrMo$; measd *m/z* 644.1338. Anal. Calcd for $C_{18}H_{32}O_3B_4NIrMo$: C, 33.68; H, 5.03. Found: C, 33.61; H, 4.99. $^{11}B\{^1H\}$ NMR (C_6D_6; peaks are too broad to resolve the ^nJ(B,H)

(34) Macias, R.; Fehlner, T. P.; Beatty, A. M. *Organometallics* **2004**, *23*, 2124.

coupling): δ 46.6 (s, 1B), 8.6 (s, 1B), −4.3 (s, 1B), −5.7 (s, 1B). $^1H\{^{11}B\}$ NMR (C_6D_6): δ 6.74 (s, 1H, BH_t), 3.81 (s, 1H, BH_t), 3.51 (s, 1H, BH_t), 3.03 (s, 1H, BH_t), 1.78 (s, 15H, Cp*), −0.21 (q, ^nJ(H,H) = 7 Hz, 1H, BHB), −3.33 (quit, ^nJ(H,H) = 7 Hz, 1H, BHB), −3.61 (s, 1H, BHB), −9.39 (t, ^nJ(H,H) = 7, 1H, MoHB).

Synthesis of [{Cp*Ir}{$(CO)_3(NH_3)$Mo}B_4H_8] (7). A 46 mg portion (0.121 mmol) of [Cp*IrB_4H_{10}] (**1**) was treated with 35 mg (0.121 mmol) of [{η^6-*o*-$(C_6H_4)(CH_3)_2$}Mo$(CO)_3$] in 2 mL of THF. After 30 min of stirring at room temperature under argon, 2 mL of NH_3 was condensed in the reaction flask at −70 °C. The initial orange solution turned yellow. The reaction mixture was stirred until it reached room temperature. The solvent was evaporated to dryness, the residue dissolved in CH_2Cl_2, and this mixture filtered through silica gel, giving a bright yellow solution. The solvent was evaporated to dryness and the yellow residue examined by NMR. Crystallization in hexane afforded 25 mg (0.043 mmol, 36%) of yellow [1-Cp*-2,2,2-$(CO)_3$-2-(NH_3)-*nido*-1,2-$IrMoB_4H_8$] (**7**). IR (KBr): 2524 (m, ν_{BH}), 2465 (m, ν_{BH}), 2427 (s, ν_{BH}), 1967 (vs, ν_{CO}), 1879 (vs, ν_{CO}), 1790 (vs, ν_{CO}), 1209 (m), 1027 (m), 910 (m). HR-MS (FAB): *m/z* 579.0968 (M^+ − H), calcd for $C_{13}H_{26}O_3NB_4IrMo$; measd *m/z* 579.0958. ^{11}B NMR (C_6D_6): δ 44.7 (d, 141 Hz, 1B), 7.5 (t, 95 Hz, 1B), −4.4 (d, 1B), −5.5 (d, 1B). $^1H\{^{11}B\}$ NMR (C_6D_6): δ 6.65 (s, 1H, BH_t), 3.28 (t, 6 Hz, 1H, BH_t), 2.97 (t, 6 Hz,1H, BH_t), 2.87 (t, 6 Hz, 1H, BH_t), 1.54 (s, 15H, Cp*), 0.09 (br. s, 3H, NH_3), −0.38 (q, ^nJ(H,H) = 6 Hz, 1H, BHB), −3.41 (quit, ^nJ(H,H) = 7, 1H, BHB), −3.60 (s, 1H, BHB), −7.98 (t, ^nJ(H,H) = 7, 1H, MoHB).

Compound **7** decomposed overnight in a CH_2Cl_2/hexane solution at 4 °C under an argon atmosphere, giving a brown precipitate and the tetracarbonyl derivative **2**.

Reaction of [1-Cp*-2,2,2-$(CO)_3$-2-(NCC_6H_5)-*nido*-1,2-$IrMoB_4H_8$] (5) with PPh_3=CHC$(O)_2$Me. A 95 mg portion (0.25 mmol) of [Cp*IrB_4H_{10}] was treated with 71 mg (0.25 mmol) of [{η^6-*o*-$(C_6H_4)(CH_3)_2$}Mo$(CO)_3$] in THF. After 30 min, 0.3 mL of benzonitrile was added and the reaction mixture stirred for 1 h. The solvent was evaporated to dryness, the residue dissolved in CH_2Cl_2, and this solution filtered through silica gel to give a bright yellow solution of the bezonitrile derivative **5**. The solvent was reduced in volume, and **5** was treated with 84 mg (0.25 mmol) of Ph_3P=CHC$(O)_2$Me. The reaction mixture was stirred for 1 h at room temperature. After this time, the solvent was evaporated to dryness and the residue extracted with hexane to give a yellow solution and an orange precipitate. The hexane-soluble fraction contained [Cp*IrB_4H_{10}], [Cp*IrB_3H_8], and **3**, whereas the insoluble residue was comprised mainly of **5** and a new species which exhibits the same NMR pattern as the molybdairidahexaborane series [1-Cp*-2,2,2-$(CO)_3$-2-(L)-*nido*-1,2-$IrMoB_4H_8$] (L = CO, THF, PPh_3, N≡CC_6H_5, C≡NBu, NH_3). We propose that the new species is the ylide derivative [Cp*$Ir(CO)_3$(Ph_3-$PCHCO_2Me$)MoB_4H_8] (**8**). HR-MS (FAB): *m/z* 896.1826 M^+, calcd for $C_{34}H_{42}O_5PB_4IrMo$; measd *m/z* 896.1845. $^{11}B\{^1H\}$ NMR (C_6D_6; peaks are too broad to resolve the ^nJ(B,H) coupling): δ 44.4 (1B), 8.4 (s, 1B), −5.0 (2B). $^1H\{^{11}B\}$ NMR (C_6D_6): δ 7.60−7.55 (m, C_6H_5), 7.00−6.94 (m, C_6H_5), 4.00 (d, ^1J(H,P) = 19 Hz, 1H, $PPh_3CHCO_2CH_3$), 3.76 (s, 3H, BH_t), 3.17 (s, 3H, PPh_3-$CHCO_2(CH_3)$), 1.92 (s, 15H, Cp*), −0.05 (s, 1H, B−H−B), −3.12 (s, 1H, BHB), −3.39 (s, 1H, BHB), −6.14 (s, 1H, MoHB). $^{31}P\{^1H\}$ NMR (C_6D_6): 18.4 (br s).

Separation of the reaction mixture was not possible by chromatographic means; therefore, we subjected the system to crystallization in CH_2Cl_2/hexane at −40 °C. However, after several days the intensity of the concentration of the ylide derivative decreased and that of the tetracarbonyl analogue increased, indicating that the former decomposes under the conditions of crystallization.

Acknowledgment. This work was supported by the National Science Foundation (Grant Nos. CHE 9986880 and CHE 0304008).

Supporting Information Available: Text and tables giving X-ray diffraction details, atomic coordinates, bond lengths and angles, isotropic and anisotropic displacement parameters; crystal data are also available as CIF files. This material is available free of charge via the Internet at http://pubs.acs.org.

OM049308F